DIRECT AND INDIRECT OBSERVATIONS OF LOCAL DEFORMATION PROPERTIES OF SAND SPECIMEN IN UNDRAINED TORIONAL SHEAR TESTS

The University of Tokyo, Student Member ○Chuang ZHAO
The University of Tokyo, Fellow Member Junichi Koseki

1. INTRODUCTION

The deformation of soil specimens in laboratory tests, such as triaxial tests, torsional shear tests and plane strain compression tests, may not be uniform during loading. Therefore, deformation measured at the boundaries of specimen will not be a valid parameter to present the behavior of soils. Recently, a procedure to evaluate directly the local deformation properties of sand specimens through a transparent membrane was developed. Particle Image Velocimetry (PIV) was implemented to sand specimens by adding colored sand speckles in the undrained cyclic triaxial tests. Due to the advantages over triaxial apparatus, it is required to establish a proper methodology in torsional shear tests for directly evaluating the local deformations of sand specimens. Under such circumstances, this paper investigates the local deformation properties of silica sand specimens in undrained torsional shear tests by a similar evaluation procedure with triaxial tests (Zhao et al., 2016 and 2017).

2. TEST MATERIALS

The materials employed in current research were mixed colored silica sand with white and black colors. These two colored silica sand had the same physical properties, with a mean particle size of 0.52 mm, a uniformity coefficient of 2.0, a gradation coefficient of 0.92 and a specific gravity of 2.65. The maximum and minimum void ratios were measured at 1.085 and 0.659, respectively.

3. APPARATUS AND TEST PROCEDURE

A torsional shear apparatus was employed in present study. Mixed silica sand specimen with an outer diameter of 200 mm, inner diameter of 120 mm and a height of 300 mm was set in a pressure cell and was loaded in the torsional and vertical directions independently. In all tests, hollow cylindrical specimens were prepared by air pluviation method through which homogeneous specimens could be obtained with constant relative density of 50%-55%. Subsequently, the double vacuuming method was applied for the saturation process by which a high B value larger than 0.96 could be obtained. The specimens were consolidated to an isotropic effective stress state of 100 kPa with a back pressure of 200 kPa. After that, undrained cyclic torsional loading with a constant single amplitude of shear stress was implemented while the vertical displacement was not allowed. The shear strain rate was controlled to be 0.025%/min and cyclic loading was terminated when the double amplitude of shear strain reached 15%.

In addition, image analysis was applied in these tests for capturing the local deformations during loading through a transparent membrane. Before specimen preparation, black colored latex dots were pasted on the membrane surface as shown in Fig.1, with an interval of 5 mm both in vertical and horizontal directions. The dots on membrane were traced for the indirect evaluation of local deformations. On the other hand, sand particles seen clearly through the transparent membrane could be used for direct evaluation. Moreover, four LED lights were pasted at the outside surface of cell to create a homogeneous brightness on the surface of specimen. The side view of specimen was recorded by using a digital camera with a resolution of 4912*7360 pixels. A commercial software named Move-tr 2D was used to obtain the coordinates of dots on membrane and patterns of sand particles, respectively. A coordinate correction procedure was implemented to eliminate the distortion effects from cylindrical shape of specimen and other factors. Finally, local strains in four grid nodes were analyzed and plotted by MATLAB.

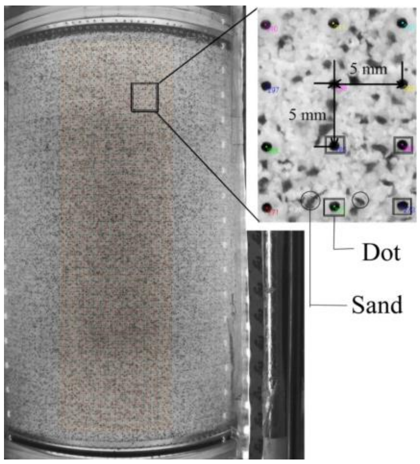

Fig. 1 Transparent membrane and dot setting

4. TEST RESULTS

4.1 Behavior during Undrained Cyclic Loading

Observed behavior in test 3 where the specimen was subjected to a cyclic stress ratio of 0.23 is shown in Figs. 2(a) through 2(c). In Fig. 2(b), the effective stress path is shown in terms of the shear stress and the current effective mean principal stress. The cyclic mobility was observed in the figure where the effective stress recovered repeatedly after showing zero effective stress state. It was accompanied with a significant development of double amplitude of shear strain as shown in Fig. 2(c).

Keywords: liquefaction, silica sand, image analysis, local deformations and torsional shear tests
Contact address: Geo-lab, 7-3-1 Hongo, Bunkyo-ku, Tokyo, 113-8656, Japan, Tel: +81- 3-5841-6123

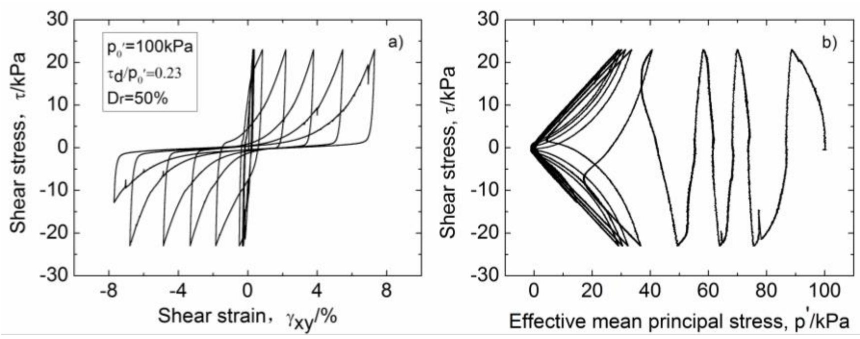

Fig. 2 Test results on silica sand

4.2 Image Analysis Results

Fig. 3 displays the local shear strain distributions of specimen at steps 388 and 2685 when the shear strains measured by potentio-meter were -1.84% and 7.3% as shown in Fig. 2(c). The local strain distribution from traced dots on membrane was almost same with the one from sand particles patterns at step 388. However, different local strains were found between indirect and direct evaluations at step 2685. Compared with the original photo at step 2685, apparent membrane wrinkles did not occur which could be confirmed by the indirect evaluation (from dots on membrane). Therefore, these different local strains between indirect and direct evaluations indicated that the information of strain localization at step 2685 as shown in Fig. 3 might be missed by the indirect evaluation.

In order to investigate the reason for different local strains between membrane and sand specimen, several dots and adjacent sand particles were selected and analyzed. Fig. 4 shows the step histories of excess pore water pressure ratio (EPWPR) and slippage. The positive value of slippage meant that the displacement of sand particle was larger than the dot on vertically down direction. Dot on membrane and sand particle suffered the same deformation during loading before EPWPR reached unity. Subsequently, slippage between them occurred under liquefaction conditions during cyclic mobility. This phenomenon proved that the local deformations from membrane were valid before initial liquefaction. On the other hand, the indirect evaluation of local deformations could not represent the behavior of sand specimen after initial liquefaction.

As mentioned previously, nine positions from the dots and adjacent sand particles were selected randomly at the top, middle and bottom parts of specimen surface. The relationships between accumulated slippage and EPWPR of these positions are plotted in Fig. 5. Slippages were accumulated when EPWPR reached unity at each half cycle.

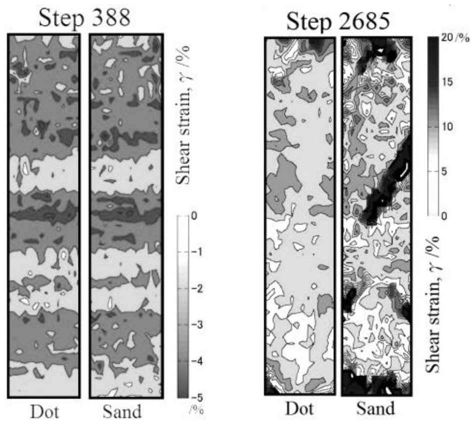

Fig. 3 Local strain distributions

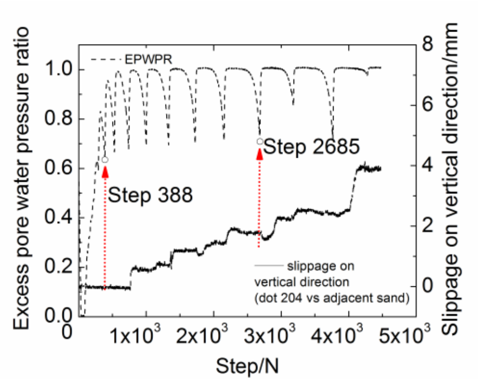

Fig. 4 Histories of excess pore water pressure ratio and slippage

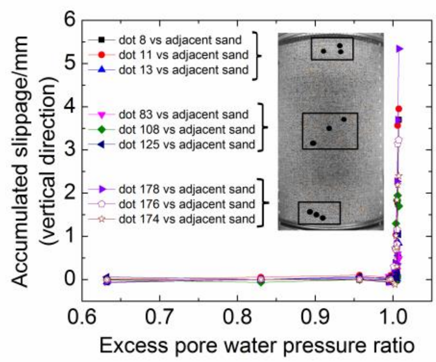

Fig. 5 Relationships between accumulated slippage and excess pore water pressure ratio

5. CONCLUSIONS

The image analysis method employed in present research could be used as a powerful tool to investigate the local deformations of sand specimen in torsional shear tests. Through the transparent membrane, local strains were measured directly and indirectly from dots on membrane and sand particles patterns, respectively. Moreover, local strains could be plotted visually and clearly by the local strain distributions. The significant leap of slippage between membrane and sand particles occurred when EPWPR reached unity at each time. Therefore, the local deformation results from indirect evaluation could not represent those from direct evaluation after initial liquefaction.

6. REFERENCES

Zhao, C., Miyashita, Y., Koseki, J.: The comparison of direct and indirect local deformations of silica sand by image analysis in triaxial liquefaction tests, Proceedings of the 18th International Summer Symposium, JSCE, 2016, pp. 39-40.
Zhao, C., Koseki, J., Miyashita, Y.: Direct and indirect local deformations of sand in undrained cyclic triaxial tests by image analysis technique, Advances in Laboratory Testing and Modelling of Soils and Shales, ISSMGE, 2017, 215-222.